EFFECT OF DIFFERENT QUATERNARY BLENDS OF DIESEL-ETHANOL-METHANOL-BUTANOL ON COMBUSTION AND SPRAY CHARACTERISTICS OF DIESEL ENGINE

by

Indranil SINHA[a,b*], Ambarish DATTA[c], and Bijan Kumar MANDAL[a]

[a]Department of Mechanical Engineering, Indian Institute of Engineering Science and Technology, Shibpur, Howrah, West Bengal, India
[b]Department of Mechanical Engineering, RamkrishnaMahato Government Engineering College, Purulia, West Bengal, India
[c]Department of Automobile Engineering, Memari Government Polytechnic, PurbaBardhaman, West Bengal, India

Original scientific paper
https://doi.org/10.2298/TSCI240212190S

The impact of different diesel-ethanol-methanol-butanol (DEMB) blends on the spray and combustion characteristics of a single-cylinder Diesel engine has been investigated. For this study, commercially available software called Diesel-RK that can predict the spray and combustion parameters has been utilized. Some experiments have also been conducted using D100 (100% pure diesel by volume) fuel at a fixed speed of 1500 rpm at peak load while maintaining the same operating conditions as the simulation. The predicted results have been validated against the experimental results obtained with D100. The results of the simulation were found to be in reasonably good agreement with those of the experiment. The analysis of the simulated results shows that the heat release rate, ignition delay and peak cylinder pressure increase for all quaternary blends, whereas the peak combustion temperature decreases at low load and increases at higher load. In terms of spray characteristics, the investigations show that quaternary alcohol blends shorten spray tip penetration and increase spray cone angle. Furthermore, as the proportion of ethanol and methanol in the DEMB blends increases, the atomized fuel droplets become smaller in diameter and the sauter mean diameter of the blends gradually drops. The authors also suggest that the quaternary blends of this present investigation have a higher potential to be used as a next-generation fuel in Diesel engine.

Key words: *methanol, ethanol, butanol, Diesel engine, diesel-RK, combustion, spray characteristics*

Introduction

In modern civilization, the diesel engine is the most suitable choice of internal combustion engine due to its lower specific fuel consumption, higher thermal efficiency, and higher power output [1]. Diesel engine is the primary source of power for the automobile, agriculture, and marine industry. However, Diesel engines have the disadvantages of higher PM, NO_x, and

*Corresponding author, e-mail: indranil323@gmail.com

unburned HC emission, which causes serious threats to the environment. The transportation sector is the major contributor to this emission. In order to control this emission different new regulations on exhaust emission from Diesel engines have been adopted. The latest BS-VI regulations for heavy-duty vehicles in India require that PM and NO_x emissions should be reduced by 50% and 89% from the BS-IV level as measured on steady-state cycles [2]. To achieve this stringent emission legislation, the compression engine has to further reduce its pollutant emissions. In this context, different organizations and researchers from various parts of the world have motivated themselves to find out the probable solution to this burning issue. To combat the emission legislation and minimize the environmental pollution caused by Diesel engines, bio-alcohols, such as ethanol, methanol, butanol and pentanol can be used in blending with mineral diesel in various proportions in compression ignition (CI) engines as supplementary fuel sources [1, 3]. It has been confirmed by different studies that oxygenated fuel additives efficiently reduce soot and exhaust PM emissions. The decrement in prototypical gas-phase soot precursor and hydroxyl (OH) molecules present in the alcohol may be the main reason behind it.

Easy production and low cost make methanol an effective choice for CI engine fuel. Methanol can be prepared from syngas, natural gas and biomass. The CO_2 hydrogenation [4] and conversion of CH_4 to methanol can be the other way to produce methanol [5]. Higher octane ratings and good explosion resistance of methanol are responsible for improving the compression ratio, which enhances thermal efficiency. Dou *et al.* [6] found that the number of soot particles gradually decreased with the increasing methanol percentage. However, due to the polarity difference, mixing of methanol and diesel bland is challenging and the fuel blend is less stable after blending. Compared with pure diesel, methanol/diesel blended fuels reduce engine brake thermal efficiency and increase HC and CO emissions [7]. Therefore, these problems greatly limit the application of methanol as an alternative fuel for Diesel engines.

Ethanol is another choice among the other lower alcohols. Ethanol has better combustion characteristics compared with methanol due to its lower latent heat of vaporization and combustion temperature. The experimental result showed by Kurre *et al.* [8] investigated that with the addition of ethanol fraction to the neat diesel, the thermal efficiency reduced slightly, and the BSFC and EGT increased. Whereas, NO_x, CO_2, HC, and CO decreased with increasing ethanol fraction in the blended fuel, and soot emissions dropped drastically. Shadidi *et al.* [9] investigated the exhaust emission characteristics of Diesel engine using a diesel-ethanol fuel blend and reported that due to the higher oxygenated nature of ethanol, the diesel-ethanol fuel blend reduces the HC and CO emissions up to 16.25% and 30.6%, respectively. Padala *et al.* [10] showed that the higher ethanol content in the fuel blends improved engine thermal efficiency, though the unburned HC, CO and NO_x emissions increased with the ethanol fraction.

Chen *et al.* [11] reported that with the increase of methanol fraction in diesel-pentanol blends, the ignition delay prolongs, combustion duration reduces, and maximum temperature increases. Nour *et al.* [12] studied the effect of ternary blends pentanol/hydrous ethanol/diesel and octanol/hydrous ethanol/diesel on the Diesel engine performance, emission, and combustion. They reported that the maximum cylinder pressures for ternary blends are lower than that of diesel. The rate of heat release at the premixed stage combustion phase is minimal but higher for the diffusion combustion zone. Ignition delay and combustion duration were found to be higher for ternary blends. Prabakaran *et al.* [13] experimentally investigated that heat release rate (HRR), maximum in-cylinder pressure, of the ternary blend was found closer to diesel at peak load for ternary blends of ethanol-diesel-butanol. Zhang *et al.* [14] numerically studied the combustion, spray, and emission characteristics of Diesel engine fueled with diesel/methanol/n-butanol blends. The study showed that ternary blends played a key role in the fuel spray

combustion processes which results in longer ignition delay, higher cylinder pressure, and higher peak HRR compared with mineral diesel.

Gomez *et al*. [15] studied the effect of diesel-biodiesel-ethanol blends on the spray macroscopic parameters in a common-rail diesel injection system. They injected different blends in a constant volume chamber and measured the spray macroscopic parameters. The results showed that blends with higher density increase spray tip penetration (STP) and less kinematic viscosity surface tension results in higher spray cone angle (SCA). Also, they predicted that an increase in the ethanol volume fraction results in a reduction of the density, kinematic viscosity, and surface tension of the diesel biodiesel-ethanol blends which concludes DB30E10 is the best blend as per stable mixing and allowed physical properties. Mo *et al*. [16] studied the effect of *n*-butanol blending on spray characteristics of soybean biodiesel in a common-rail fuel injection system at room temperature and pressure. They analyzed the spray macroscopic parameters such as STP, SCA, projected spray area, sauter mean values, *etc*. The investigation results showed that spray penetration length and SCA were almost similar for the alcohol-biodiesel blends although neat biodiesel has the longest penetration among all tested fuels.

The majority of research concentrated on exploring the impact of different types of alcohol on combustion and emission performances using different binary and ternary blends of diesel/ethanol/methanol/butanol. However, there has been a major deficiency in the studies that investigate the effects of quaternary blends of DEMB on engine combustion and spray characteristics. For the spray combustion behaviour aspect, most of the available literature is based on using a high-speed camera and an image analyzer to examine the optical diagnostic data such as STP, SCA and sauter mean diameter (SMD). However, all these investigations are experimental and involve a huge amount of time, cost and labour. To minimize this, a proper mathematical model can be very useful in the area of engine research. Keeping this in mind, the authors have made an attempt to investigate numerically the combustion and spray combustion characteristics of a CI engine using quaternary blends of ethanol, methanol and butanol. This research will help the automotive and transportation industries to develop methods for sustainable energy use and emission management.

Methodology and engine details

In this investigation, the four blends of alcohol D85E5M5B5 (85% diesel, 5% ethanol, 5% methanol, and 5% butanol by volume), D80E10M5B5 (80% diesel, 10% ethanol, 5% methanol, and 5% butanol by volume), D80E5M10B5 (80% diesel, 5% ethanol, 10% methanol, and 5% butanol by volume) and D80E5M5B10 (80% diesel, 5% ethanol, 5% methanol, and 10% butanol by volume) are used as fuels and the simulation has been carried out using a commercial software, Diesel-RK. The results obtained from the simulation are validated with experimental results using neat diesel (D100) as a working fuel. Some of the important thermo-physical properties of the different alcohols and neat diesel are presented in tab. 1 for comparison [17]. Kirloskar TV1 Diesel engine has been selected for numerical investigation at its rated condition. The engine speed, fuel injection timing, compression ratio, and fuel injection duration remain constant at 1500 rpm, 23° bTDC, 18:1, and 54.5 °CA during the simulation. The simulation incorporate a constant mass supply per cycle for a specific load and blend. During numerical simulation, the authors vary the cycle fuel mass to alter the engine loads for a particular blend. This variation in load results in significant changes in injection pressure due to the constant injection duration. Detailed specifications of Kirloskar TV1 are given in tab. 2 and fig. 1. Diesel- RK software has some in-built models for engine friction, heat release and NO_x for-

Table 1. Physical and chemical properties of different alcohols

Properties	Methanol	Ethanol	Butanol	Diesel
Molecular weight [gmol^{-1}]	32	55	74	182
Density at 40 ºC [gcm^{-3}]	0.791	0.789	0.810	0.832
Carbon content [wt.%]	37.48	52.14	65	86.13
Hydrogen content [wt.%]	12.48	13.02	13.5	13.87
Oxygen content [wt.%]	49.93	34.73	21.5	0
Cetane number	5	8	17	52
Heat of vaporization [kJkg^{-1}]	1162	918	582	272
Lower heating value [MJkg^{-1}]	19.58	26.83	36.1	42.49
Kinematic viscosity at 40 ºC [mms^{-2}]	0.58	1.13	2.22	2.72
Surface tension [Nm^{-1}]	0.02207	0.015	0.025	0.0275

Table 2. Technical specification of the engine

Make	Kirloskar
Type	4-stroke, single-cylinder
Compression ratio	18
Maximum power occurrence	3.5 kW
Bore [mm]	87.5
Stroke length [mm]	110
Connecting rod length	234 mm
Number of injector nozzles	3
Maximum injector pressure	220 bar

Figure 1. Experimental test engine

mation. The fuel gallery is to be made for the simulation after developing the engine model. In the fuel gallery, the properties of different quaternary blends have been inserted. The thermo physical properties of the different quaternary fuel blends (*i.e*, D85E5M5B5, D85E10M5B5, D85E5M10B5, and D85E5M5B10) are shown in tab. 3. The output data comprises different engine combustion data, such as cylinder pressure, cylinder temperature, ignition delay, HRR, and spray characteristics such as STP, SCA, and SMD.

Table 3. Physical and chemical properties of different quaternary blends

Properties	D85E5M5B5	D80E10M5B5	D80E5M10B5	D80E5M5B10
Density at 40 ºC [gcm^{-3}]	0.826	0.826	0.824	0.825
Carbon content [wt.%]	80.93	79.23	78.5	79.86
Hydrogen content [wt.%]	13.73	13.69	13.66	13.72
Oxygen content [wt.%]	5.31	7.04	7.80	6.39
Cetane number	45.7	43.50	43.35	43.95
Heat of vaporization [kJkg^{-1}]	362.59	395.01	407.19	378.16
Lower heating value [MJkg^{-1}]	40.09	39.30	38.94	39.62
Kinematic viscosity at 40 ºC [mms^{-2}]	2.50	2.42	2.40	2.48
Surface tension [Nm^{-1}]	0.0264	0.0258	0.0262	0.0263

Numerical modelling

Models used to evaluate various combustion parameters are presented briefly in the next sections.

Heat release model

The Diesel-RK program uses the multi-zone combustion model [18]. There are four main phases involved in the heat release process. The first phase is the ignition delay is govoerned using modified Tolstov's equation [19]:

$$\tau = 3.8\times10^{-6}\left(1-1.6\times10^{-4}n\right)\sqrt{\frac{T}{p}}\exp\left(\frac{E_a}{8.312T}-\frac{70}{CN+25}\right) \tag{1}$$

where E_a [kJmol^{-1}], T [K], p [bar], and CN represent the apparent activation energy, charge temperature, pressure, and fuel cetane number, respectively. The premixed combustion period is the second phase of the HRR:

$$\frac{\mathrm{d}x}{\mathrm{d}\tau} = \phi_o\left[A_0\left(\frac{m_f}{V_i}\right)(\sigma_{ud}-x)(0.1\sigma_{ud}+x_0)\right]+\phi_1\left(\frac{\mathrm{d}\sigma_u}{\mathrm{d}\tau}\right) \tag{2}$$

The HRR for the mixing-controlled combustion phase is given by:

$$\frac{\mathrm{d}x}{\mathrm{d}\tau} = \phi_1\left(\frac{\mathrm{d}\sigma_u}{\mathrm{d}\tau}\right)+\phi_2\left[A_2\left(\frac{m_f}{V_c}\right)(\sigma_u-x)(\alpha-x)\right] \tag{3}$$

The final stage of the HRR occurs after the fuel injection. It is computed using the following relation:

$$\frac{\mathrm{d}x}{\mathrm{d}\tau} = \varphi_3 A_3 K_T(1-x)(\xi_b\alpha-x) \tag{4}$$

In those equations, it is assumed that $\varphi_0 = \varphi_1 = \varphi_2 = \phi$ which describes the completeness of fuel vapour combustion in the zones. The m_f is the fuel mass per cycle, V_i and V_c are cylinder volumes at injection timing and at TDC, respectively, σ_{ud} and σ_{u} are fuel fractions evaporated during the ignition delay period and up to the current moment, respectively, A_0, A_1, A_2, and A_3 are empirical factors depending on engine speed, swirl intensity.

Spary model

The fuel injectors of modern diesel engines produce the fuel spray with approximately the same average size of droplets (denoted as d_{32}) which can be determined using the Sauter's equation [19]:

$$d_{32} = 1.7d_{\mathrm{orif}}\left(\mathrm{We}\frac{\rho_{\mathrm{g}}}{\rho_{\mathrm{l}}}\right)^{-0.266} M^{0.0733} \tag{5}$$

where d_{orif} is the diameter of the nozzle orifice, ρ_l and ρ_g are the density of liquid fuel and density of ambient gas, respectively, We and M are the Weber number and squared Ohenzorge number, respectively. It is needed to note that criterion M is equivalent to the Weber number divided by the square of the Reynolds number. The mathematical expressions for the mentioned two numbers are as:

$$\mathrm{We} = \frac{V_{\mathrm{inj}}\rho_{\mathrm{l}}d_{\mathrm{orif}}}{\sigma_{\mathrm{l}}} \tag{6}$$

$$M = \frac{\mu_l^2}{\rho_l d_{\text{orif}} \sigma_l} \tag{7}$$

where σ_l is the surface tension coefficient of liquid fuel, μ_l – the dynamic viscosity of fuel liquid, V_{inj} – the injection velocity. The injection velocity V_{inj} is determined by the well-known Bernoulli's equation for inner tube flow and it is given by:

$$V_{\text{inj}} = \sqrt{\frac{2(p_{\text{in}} - p_{\text{amb}})}{\rho_l}} \tag{8}$$

where p_{in} and p_{amb} are the injection pressure and ambient pressure, respectively.

The STP is calculated using the following empirical correlations developed by Lyshevsky and modified by Razleytsev see in [20]:

$$L_{tip} = 10.37 d_{\text{orif}} \text{We}^{0.25} M^{0.4} \left(\frac{\rho_l}{\rho_g}\right)^{-0.6} \left(\frac{\tau_s}{\tau_b}\right)^{0.7} \exp\left(\frac{-0.2\tau_s}{\tau_b}\right), \text{ if } \tau_s \le \tau_b \tag{9}$$

$$L_{tip} = \frac{d_{\text{orif}}^{0.5} V_{inj_{\text{ave}}}^{0.5} \rho_g^{0.5} \text{We}^{0.105} M^{0.08} \tau_s^{0.5}}{2.63 \rho_l^{0.5}}, \text{ if } \tau_s > \tau_b \tag{10}$$

where $V_{inj\text{ave}}$ is the average injection velocity, τ_s – the current time after the start of injection, and τ_b – the jet breakup time and calculated as:

$$\tau_b = \frac{500 d_{\text{orif}} \rho_g^{0.2} \text{We}^{0.32} M^{0.64}}{V_{inj_{\text{ave}}} \rho_l^{0.2}} \tag{11}$$

The expression for SCA β is written as same as Markov *et al*. [20]:

$$\tan\left(\frac{\beta}{2}\right) = 0.008 \text{We}^{0.32} \Big/ M^{0.07} \left(\frac{\rho_g}{\rho_l}\right)^{0.5} \left(\frac{\rho_l d_{\text{orif}}^3}{\sigma_l \tau_s^2}\right)^{0.12}, \text{ if } \tau_s > \tau_b \tag{12}$$

$$\tan\left(\frac{\beta}{2}\right) = 0.0075 \text{We}^{0.32} \Big/ M^{0.07} \left(\frac{\rho_g}{\rho_l}\right)^{0.5} \left(\frac{\tau_s}{\tau_b}\right)^{0.24} \exp\left(\frac{0.7\tau_s}{\tau_b}\right), \text{ if } \tau_s \le \tau_b \tag{13}$$

Determination of fuel properties

A set of calculations based on the basic properties of pure fuels has been used to establish the properties of the quaternary blends of DEMB. The densities, ρ_b, cetane numbers, CN_b, and lower heating values, LHV_b, are calculated using the Kay Mixing Rule. The kinematic viscosities of the quaternary blends are computed using the Refutas equation [21] and the Arrhenius mixing rule:

$$CN_b = \sum_{i=1}^{4} Y_i CN_i \tag{14}$$

$$\rho_b = \sum_{i=1}^{4} Y_i \rho_i \tag{15}$$

where Y_i is the volumetric mixing ratio of fuel components, CN_b – the cetane number of the blend, and CN_i – the cetane number of each fuel component.

The following equation is used to calculate the kinematic viscosities of the different quaternary blends according to the Arrhenius mixing rule:

$$\ln \lambda_b = \sum_{i=1}^{4} Y_i \ln \lambda_i \tag{16}$$

where λ_b [mm^2] is the kinematic viscosity of the blend and λ_i – the known kinematic viscosity of each fuel component.

Another method for calculating kinematic viscosities is the Refutas equation. Refutas equation consists of three steps. The first step is to calculate the viscosity blending index, VBI_i, of each fuel component:

$$VBI_i = 14.534 \times \ln\left[\ln\left(\eta_i + 0.8\right)\right] + 10.975 \tag{17}$$

The next step was to calculate the VBI of the blend, VBI_b, using:

$$VBI_b = \sum_{i=1}^{4} \left(Y_i \times VBI_i\right) \tag{18}$$

The final step is to determine the kinematic viscosity of the blend according to:

$$\lambda_b = \mathrm{e}^{e\left[(VBI_b - 10.975)/14.534\right]} - 0.8 \tag{19}$$

In this investigation, the authors use the Arrhenius Mixing rule to calculate the kinematic viscosity due to its meaningful theoretical substantiation and satisfactory accuracy. Dynamic viscosity, μ_b, lower heating value, LHV_b, and surface tension, σ, of the quaternary blends are calculated using:

$$\mu_b = \sum_{i=1}^{4} \left(\lambda_i \times \rho_i \times Y_i\right) \tag{20}$$

$$LHV_b = \frac{\sum_{i=1}^{4} Y_i \rho_i LHV_i}{\sum_{i=1}^{4} Y_i \rho_i} \tag{21}$$

$$\sigma_b = \left(49.6\rho_b - 14.92\right) \times 10^{-3} \tag{22}$$

where σ_b represents the fuel blend surface tension and ρ_b represents the fuel blend density.

Model validation

In order to evaluate the validity of the model, obtained simulation results have been compared with experimental results maintaining the same operating parameters. An experimental investigation is conducted on a mono-cylinder four-stroke Diesel engine using neat diesel at a maximum load of 3.5 kW. Comparison has been carried out for combustion of the characteristics using D100 (100% neat diesel by vol.). Figures 2 and 3 compare the combustion parameters such as cylinder pressure and HRR at peak load in relation to the crank angle. The investigators found respectable agreement between the numerical data and experimental data for HRR and cylinder pressure at peak load. The deviation of error is found to be less than 5% for cylinder pressure and HRR for peak load conditions. The results showed numerical values

agreed with the experiment. Therefore, the numerical model can accurately predict the performance; spray macroscopic, combustion and emission behavior of the engine.

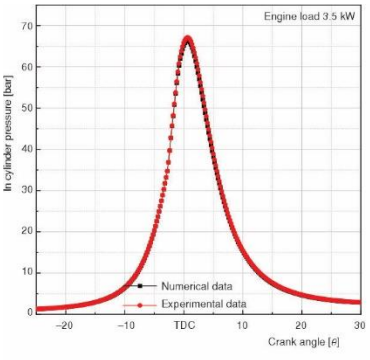

Figure 2. Variation of cylinder pressure with the crank angle for D100

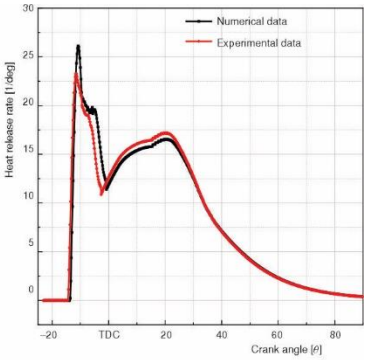

Figure 3. Variation of HRR with the crank angle for D100

Error and experimental uncertainty analysis

To improve accuracy, it is imperative to perform an uncertainty analysis of the test setup. To obtain precise results, the experiment was run six times. One way to define experimental uncertainty is as the potential value that an error could have. Let u_1, u_2,...,u_n be the uncertainties in the independent variables and U_R be the uncertainty in the final result. The results are then used to calculate uncertainty using the root mean square method [22]. The total experimental uncertainty is represented as:

$$U_R = \left[\left(\frac{\delta R}{\delta L_1}u\right)^2 + \left(\frac{\delta R}{\delta L_2}u_2\right)^2 + \ldots + \left(\frac{\delta R}{\delta L_n}u_n\right)^2\right]^{1/2}$$

where

$$R = R\left(L_1, L_2, \ldots, L_n\right)$$

Uncertainty percentage = [(flow rate of fuel)^2 + (lower heating value)^2 + (crank angle shaft encoder)^2 + (load cell)^2 + (pressure sensor)^2 + (engine speed sensor)^2 + (temperature sensor)^2]$^{1/2}$. The overall uncertainty of the experiments was found to be ± 1.76 % which is in the acceptable range.

Result and discussion

In this section, the results related to combustion and spray characteristics have been presented.

Combustion parameters

The combustion characteristics of quaternary fuel blends have been described in terms of various combustion parameters such as cylinder pressure, cylinder temperature, ignition delay and HRR.

Cylinder pressure

The variations of in-cylinder pressure at different load conditions for various quaternary blends of DEMB are plotted in fig. 4. The higher percentage of alcohol in the blended fuel

shows higher cylinder peak pressure. The position of the peak pressure for quaternary blended fuel has shifted towards right from TDC and it denotes the retarded start of combustion. Notably, D85E5M5B5 exhibits the highest peak cylinder pressure of 56.68 bar and 75.62 bar at 0.5 kW and 3.5 kW, respectively, followed by D80E10M5B5, D80E5M10B5, D80E5M5B10, and D100. Furthermore, an increase in load is accompanied by an increase in cylinder pressure. In quaternary blends butanol is used as a co-solvent also the addition of methanol and ethanol in different proportions improves the combustion behaviour. Alcohol fuels are oxygenated in nature and they have a higher combustion speed which promotes improved combustion. Also, the atomization processes of alcohol diesel blends are superior because fuel droplets are further broken down into smaller particles during the secondary atomization which is known as the micro explosion. At comparatively higher loads more fuel injection and less oxygen availability, lower cetane number, and high latent heat of evaporation may be the other reasons behind the higher peak cylinder pressure. Also, it is observed that the main variation is at the peak as well as at the early stage of combustion.

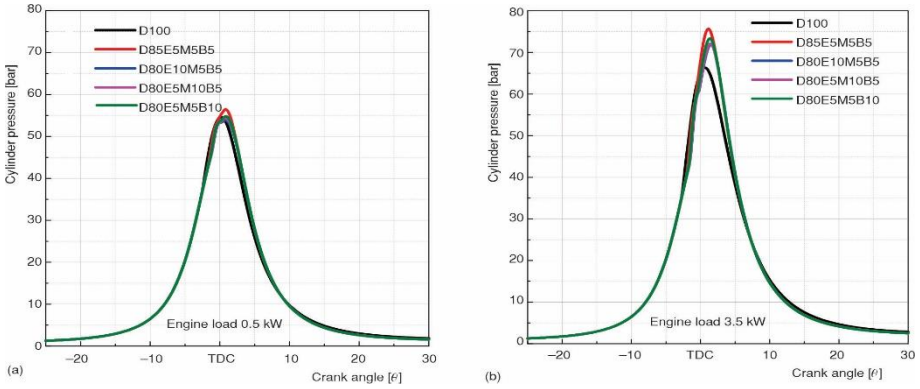

Figure 4. In-cylinder pressuresfor different fuels at; (a) 0.5 kW and (b) 3.5 kW loads

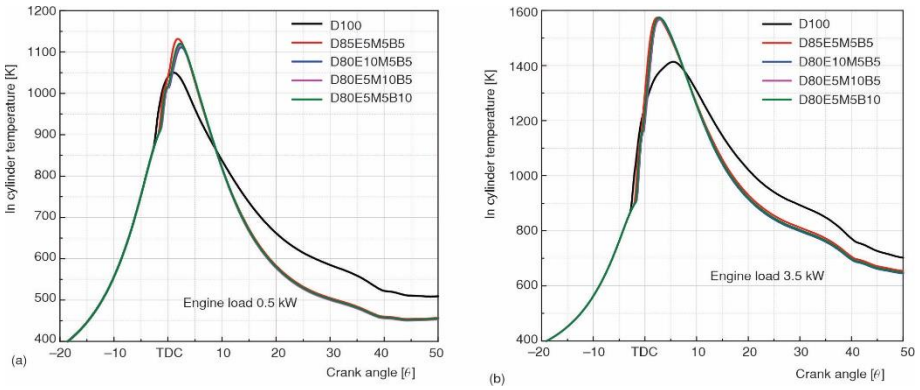

Figure 5. In-cylinder temperature at different fuels at; (a) 0.5 kW and (b) 3.5 kW loads

Cylinder temperature

Figure 5 shows the variation of combustion temperature at varying loads for quaternary blends of DEMB. At a lower load, D100 exhibited the highest temperature, followed by D85E5M5B5, D80E5M5B10, D80E10M5B5, and D80E5M10B5. At a lower load (0.5 kW) as

the alcohol proportion in the blend increases, the cylinder temperature decreases. This trend arises due to the high latent heat of the vaporization of methanol and ethanol during the evaporation process, resulting in more heat being transferred to the cylinder wall. However, at a higher load, mostly methanol and ethanol affect engine cylinder temperature due to their higher oxygen content compared to diesel fuel. As the alcohol fraction increases, the oxygen level in the blend enhances combustion inside the cylinder, leading to a higher cylinder temperature. For instance, at 100% engine load (3.5 kW), pure diesel results in the lowest peak cylinder temperature, followed by the other quaternary blends with temperature increments ranging from 1.61% to 2.87%.

Ignition delay

The ignition delay period is the time interval between the start of the combustion and the commencement of fuel injection. Ignition delay is an important factor in engine combustion and it depends on the cetane number of the fuel. Figure 6 shows the comparisons of ignition delay for diesel and different tested fuels for diesel/ethanol/methanol/butanol fuel blends with respect to brake power. It is found that ignition delay is longer with diesel-alcohol quaternary blends compared to the mineral diesel. The iginition delays are noted to be 14.17 ºCA at 100% load for D100, 22.49 ºCA at peak load for D80E5M5B5, 27.28 ºCA at full load condition for D80E10MB5, 25.61 ºCA at peak load for D80E5M10P5 and 28.19 ºCA at full load condition for D80E5M5B10. The increase in alcohol fraction in the blended fuels decreases the cetane number of the fuel blends which in turn results in a longer ignition delay. Higher methanol blended fuel has lower cetane no compared to the other alcohol in quaternary blends. Longer ignition delay leads to burning of larger amount of fuel at premixed stages of combustion which causes a higher heat release in pre-mixed phase.

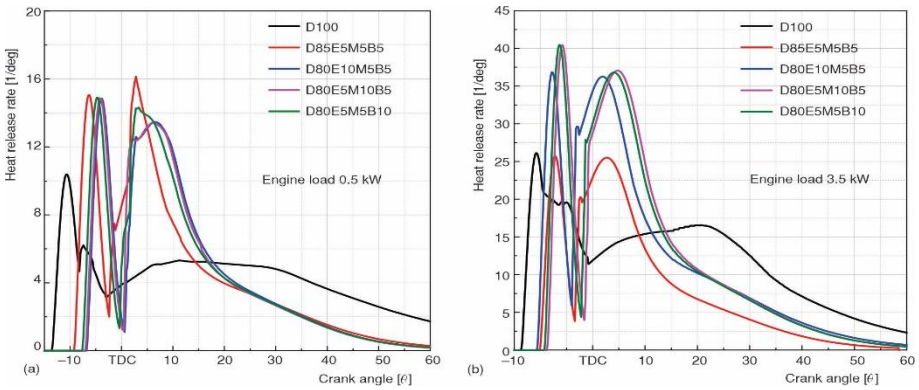

Figure 6. Heat release rate at different fuels at; (a) 0.5 kW and (b) 3.5 kW loads

Heat release rate

The HRR J/ºCA with respect to crank angle at different load condition (0.5 kW and 3.5 kW) for DEMB blends depicts in fig. 7. The maximum in-cylinder HRR for mineral diesel (D100), D85E5M5B5, D80E10M5B5, D80E5M10B5, and D80E5M5B10 are 26.14, 36.71, 40.37, 40.51 and 40.53, respectively, at peak load. It is found that both maximum HRR (pre-mixed and diffusion combustion stage) for quaternary blended fuels are much higher than that of mineral diesel. It is also noted that the HRR curves are steeper with a higher percentage of

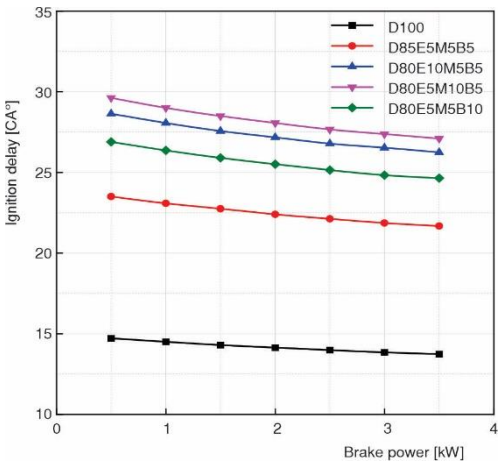

Figure 7. Ignition delay at different engine loads

butanol in the quaternary blend. Increasing the amount of ethanol and methanol in fuel blends also leads to a higher HRR because it improves how the fuel mixes and adds more oxygen to it. A higher oxygen percentage of the fuel blends enhances the combustion speed and decreases the combustion duration. Mainly the lower CN and high latent heat of ethanol and methanol are held responsible for this kind of behavior. The low CN increases the ignition delay period and as a result, the fuel accumulation is also higher and higher premixed combustion is observed. Therefore HRR increases maximum for maximum methanol addition. It can be seen that HRR retard away from the TDC with an increase in the alcohol percentage for all quaternary blends for lower and higher load. It can be said that longer ignition delay and a higher amount of premixed gas cause the first peak HRR and a higher oxygen percentage in blends and a greater no of hydroxyl radicals is the reason behind the second higher peak HRR.

Spray characteristics

Fuel spray has a huge impact on engine combustion. Better spray quality leads to better atomization which enhances the combustion rate and reduces the particulate matter emission from the Diesel engine. Thus, it is essential to investigate the spray quality of the quaternary blends of DEMB. The numerical results obtained from simulation and macroscopic spray parameters have been studied during the investigation which includes SCA, STP, and SMD. Figure 8 depicts a sequence of image acquired during the injection at peak load.

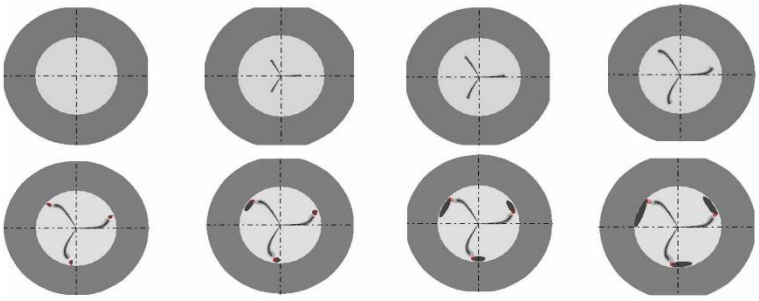

Figure 8. Spray visualization during the injection process at different crank angle

Sauter mean diameter

The SMD can be defined as the diameter of the droplet whose volume-to-surface area ratio is equal to that of the spray. The SMD of the atomized droplets is denoted as d_{32}. The SMD, mostly used to evaluate the quality of the spray and it is also one of the crucial parameters in the combustion process calculation. The variations of SMD of the different quaternary blends of DEMB blends at engine load are shown in fig. 9. The decreasing trend of SMD with respect

to the engine load is observed for diesel and all quaternary blends.The probable reason for decreased SMD with increasing brake power may be that when an engine operates under a higher load, it generally requires more fuel to combust and produce power. This can lead to higher fuel injection rates and potentially finer atomization of the fuel. Finer atomization typically results in smaller droplets or particles in the spray, leading to a decrease in the SMD. During numerical simulation, as the engine load increases, the SMD decreases with an increase in fuel injection pressure. This can be explained by the increased injection velocity caused by the increased fuel injection pressure. Additionally, the use of a larger nozzle diameter during simulations could also contribute to a higher SMD compared to actual engine conditions. Furthermore, methanol and ethanol have lower kinematic viscosity and surface tension which results in the lower aerodynamic force. So, quaternary blends of alcohol face less difficulty in overcoming the cohesive force and are easily broken into fine droplets. This is the main reason for the lower SMD for the quaternary blend comprised of higher methanol and ethanol percentage.

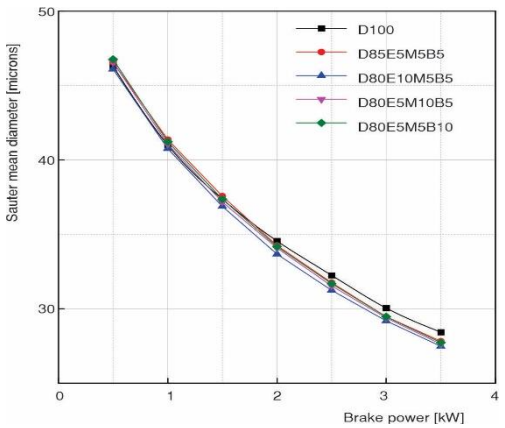

Figure 9. The SMD at different engine loads

Spray tip penetration

The STP is the length of spray along the injector's axis from the nearest point to the furthest one. During the numerical investigation, the injection duration was kept constant at 54.5 ºCA for all loads. As the injection pressure rises with the engine load, the injection velocity also increases, resulting in much higher spray penetration (almost twice) with the same injection period compared to that at lower load. The STP of different quaternary blends of DEMB at different injection times are shown in fig. 10. It is observed that the initial high velocity causes

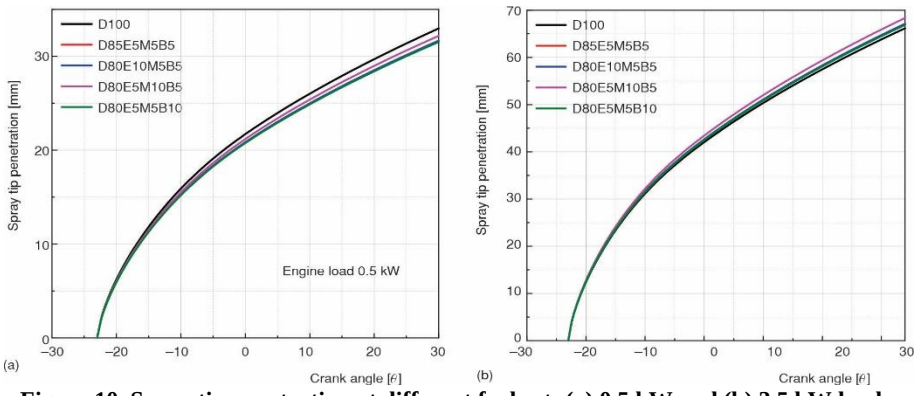

Figure 10. Spray tip penetration at different fuels at; (a) 0.5 kW and (b) 3.5 kW loads

a rapid rate of STP for the initial phase. In the later part, there was air resistance due to the air disturbance and entrainment effect, which caused a reduction in the increasing rate of STP. Quaternary fuel blends exhibited slightly lower STP due to the reduced surface tension and

kinematic viscosity of methanol and ethanol. At lower surface tension and kinematic viscosity, a fuel droplet loses its size and deforms, eventually the STP is decreased. Also, the low density of the quaternary fuel blends decreased the STP because it reduced the growth of the mass flow rate. As a result, it causes less force to be applied to the surrounding air and creates difficulties in smooth flow.

Spray cone angle

The SCA is defined as the angle between two lines connecting the nozzle tip and two half-penetration points on the spray boundary. Figure 11 shows the variation of SCA at various loads as a function of time after the start of injection for different quaternary blends of DEMB. In the actual simulations, the injection pressure varies depending on the engine load for a particular blend. As the injection pressure rises with the engine load, it leads to a higher injection velocity, which explains the observed increase in penetration and SCA at higher loads despite the constant injection duration. The SCA decreases rapidly at the beginning of the injection and after it reaches a minimum, it converges to a relatively stable value. The main reason for this is that at the initial stage, the droplets on the boundaries become smaller and diffuse easily, resulting in a decreasing trend of SCA for all quaternary fuels. After the initial period, the spray broke up into fine droplets, which resulted in stable SCA. Finally, for all the quaternary blends of DEMB, SCA increases marginally due to its low kinematic viscosity and surface tension. Increment in the spray instability may be the main reason that leads to the greater atomization of the spray.

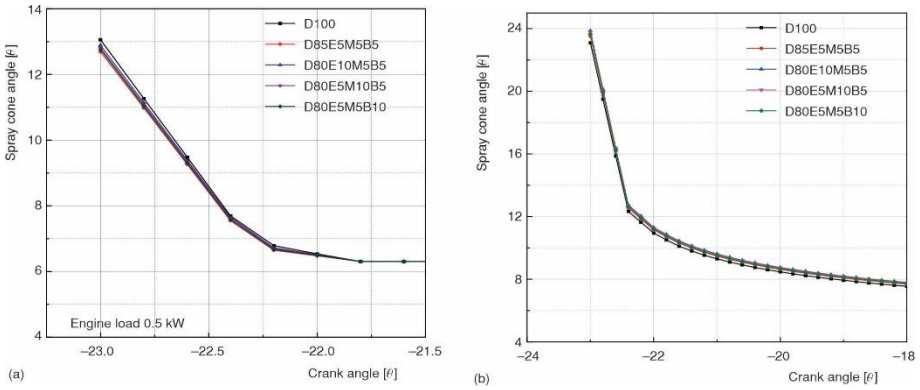

Figure 11. Spray cone angle at different fuels at; (a) 0.5 kW and (b) 3.5 kW loads

Conclusions

During the investigation, the authors studied the effect of DEMB blends using the Diesel-RK simulation tool on engine combustion and spray combustion parameters. The study was conducted at different engine loads (0.5 kW to 3.5 kW) using different quaternary blends. The simulated results were validated with experimental results using pure diesel as the base fuel. Results show good agreement between simulated results and experimental results.

At low loads, the combustion temperature for DEMB blends decreases due to the higher LHE of methanol and ethanol. On the other hand, the maximum combustion temperature rises with increasing load. A longer ignition delay period is the outcome of the alcohol's lower cetane number, and this effect is particularly noticeable in blends containing pentanol and

diesel. When comparing all quaternary blends of DEMB to neat diesel, there is an increase in both the peak pressure rise and the instantaneous HRR.

The density, kinematic viscosity, and surface tension of the blend decrease as the alcohol content increases. Fuel density influences STP. A decrease in these qualities results in lower STP. A decrease in surface tension and kinematic viscosity results in fuel droplets being more easily deformed and ruptured. The fuel's surface tension and kinematic viscosity both have an impact on the SCA. An increase in SCA results from these two properties' decline in value. For various DEMB blends, there is no discernible difference in STP. These findings suggest that the spray macroscopic parameters are not significantly affected by the characteristics of the fuels. In summary, DEMB blends have great potential to be used as a next-generation fuel without any engine modification and they also have the capability to address major issues like energy insecurity and ecological degradation.

References

[1] Dogan, O., The Influence of N-Butanol/Diesel Fuel Blends Utilization on a Small Diesel Engine Performance and Emissions, *Fuel, 90* (2011), 24, pp. 67-72
[2] ***, International Council on Clean Transportation, https://theicct.org
[3] Yao, M., *et al*., Experimental Study of N-Butanol Additive and Multi-Injection on HD Diesel Engine Performance and Emissions, *Fuel, 89* (2010), 9, pp. 2191-2201
[4] Kar, S., *et al*., Advances in Catalytic Homogeneous Hydrogenation of Carbon Dioxide to Methanol, *Journal of CO_2 Utilization, 23* (2018), Jan., pp. 212-218
[5] Prakash, C. B., *et al*., The Direct Conversion of Methane to Methanol by Controlled Oxidation, *Chemical Reviews, 85* (1983), 4, pp. 235-244
[6] Dou, Z., *et al*., Experimental Study of the Effect of Engine Parameters on Ultrafine Particle in Diesel/Methanol Dual Fuel Engine, *Fuel, 192* (2017), Mar., pp. 45-52
[7] Wei, J., *et al*., Impact of Aluminium Oxide Nanoparticles as an Additive in Diesel-Methanol Blends on a Modern DI Diesel Engine, *Applied Thermal Engineering, 185* (2021), 116372
[8] Kurre, S. K., *et al*., Experimental Study of the Performance and Emission of Diesel Engine Fueled with Blends of Diesel-Ethanol as an Alternative Fuel, *Biofuels, 6* (2015), 3-4, pp. 209-216
[9] Shadidi, B., *et al*., The Influence of Diesel-Ethanol Fuel Blends on Performance Parameters and Exhaust Emissions: Experimental Investigation and Multi-Objective Optimization of a Diesel Engine, *Sustainability, 13* (2021), 5379
[10] Padala, S., *et al*., Ethanol Utilisation in a Diesel Engine Using Dual-Fuelling Technology, *Fuel, 109* (2013), July, pp. 597-607
[11] Chen, H., *et al*., Investigation on Combustion and Emission Characteristics of a Common Rail Diesel Engine Fueled with Diesel/N-Pentanol/Methanol Blends, *Energy, 167* (2019), Jan., pp. 297-311
[12] Nour, M., *et al*., Improvement of CI Engine Combustion and Performance Running on Ternary Blends of Higher Alcohol (Pentanol and Octanol)/Hydrous Ethanol/Diesel, *Fuel, 251* (2019), Sept., pp. 10-22
[13] Prabakaran, B., *et al*., Experimental Investigation of Ethanol-Diesel-Butanol Blends in a Compression Ignition Engine by Modifying the Operating Parameters, SAE, Technical Paper 03-11-05-0037, 2018
[14] Zhang, Z., *et al*., Investigation on the Combustion and Emission Characteristics of Diesel Engine Fueled with Diesel/Methanol/n-Butanol Blends, *Fuel, 314* (2022), 123088
[15] Corral-Gomez, L., *et al*., Effect of Diesel-Biodiesel-Ethanol Blends on the Spray Macroscopic Parameters in a Common-Rail Diesel Injection System, *Fuel, 241* (2019), Apr., pp. 876-883
[16] Mo, J., *et al*., Experimental Investigation on the Effect of n-Butanol Blending on Spray Characteristics of Soybean Biodiesel in a Common-Rail Fuel Injection System, *Fuel, 182* (2016), Oct., pp. 391-401
[17] Rajesh, Kumar, B., Saravanan, S., Use of Higher Alcohol Biofuels in Diesel Engines: A Review, *Renewable and Sustainable Energy Reviews, 60* (2016), July, pp. 84-115
[18] Kuleshov, A. S., Multi-Zone Di Diesel Spray Combustion Model and its Application for Matching the Injector Design with Piston Bowl Shape, SAE, Technical Paper 2007-01-1908, 2007
[19] Kuleshov, A. S., Multi-Zone Di Diesel Spray Combustion Model for Thermodynamic Simulation of Engine with PCCI and High EGR Level, SAE, Technical Paper 2009-01-1956, 2009

[20] Markov, V., *et al*., Numerical Analysis of Injection and Spray Characteristics of Diesel Fuel and Rapeseed Oil in a Diesel Engine, *Case Studies in Thermal Engineering, 35* (2022), 102129
[21] Atmanli, A., *et al*., Extensive Analyses of Diesel-Vegetable Oil-n-Butanol Ternary Blends in a Diesel Engine, *Applied Energy, 145* (2015), May, pp. 155-162
[22] Moffat, R. J., Contributions to the Theory of Single-Sample Uncertainty Analysis, *Journal of Fluids Engineering, 104* (1982), 2, pp. 250-258

Paper submitted: February 12, 2024
Paper revised: June 12, 2024
Paper accepted: July 1, 2024